Journal of Materials Chemistry C

PAPER

View Article Online
View Journal | View Issue

Cite this: J. Mater. Chem. C, 2014, 2, 5938

Mesoporous silica/nanoparticle composites prepared by 3-D replication of highly filled block copolymer templates†

Nicholas R. Hendricks,‡ Rohit Kothari,‡ Xinyu Wang and James J. Watkins*

Received 28th February 2014
Accepted 23rd April 2014

DOI: 10.1039/c4tc00406j

www.rsc.org/MaterialsC

The incorporation of iron platinum (FePt) nanoparticles (NPs) within the walls of mesoporous silica was achieved at high NP loadings using highly filled amphiphilic poly(ethylene oxide-*b*-propylene oxide-*b*-ethylene oxide) (Pluronic®) copolymer templates prepared by exploiting selective hydrogen bonding between the pre-synthesized nanoparticles and the hydrophilic portion of the block copolymer. The mesoporous silica/NP composites were then synthesized by means of phase selective condensation of tetraethylorthosilicate (TEOS) within the NP loaded block copolymer templates dilated with supercritical carbon dioxide ($scCO_2$) followed by calcination. The resulting mesoporous silica composites were prepared at nanoparticle loadings as high as 25 wt% relative to the template (15 wt% relative to mesoporous silica) and were characterized by electron microscopy, X-ray diffraction (XRD) and X-ray photoelectron spectroscopy (XPS). The method described in this report is general and may be applied to a variety of NPs for encapsulation within the pore walls of mesoporous silica.

1. Introduction

Nanoparticles (NPs) exhibit a number of interesting catalytic, magnetic, mechanical, electrical and optical properties that are often not observed in their bulk material counterparts.[1] To take full advantage of these unique properties, novel composite materials are being developed to incorporate functional NPs into various host matrices, such as polymers,[2,3] block copolymers,[4–6] and metal oxides.[7–10] Specifically, magnetic NPs are of considerable interest due to their application in catalysis,[11,12] data storage[13] and drug delivery.[14] Magnetic NPs of a few nanometers in diameter may display interesting superparamagnetic properties which is lost upon agglomeration. Efforts have been directed in stabilizing magnetic NPs by incorporating them into mesoporous silica as well as hollow silica spheres.[15–17] In several approaches, the loading of NPs incorporated into the silica matrix was limited by weak interactions between the NP precursors and silica matrix[17] and/or between the NPs and the template required to generate the mesoporous silica.[15,16] To further extend the development of mesoporous silica/NP composites, we employ favorable interactions between pre-synthesized NPs and block copolymer templates to achieve high NP loadings. The highly filled solid templates are then used to prepare doped mesoporous silica *via* phase selective, supercritical carbon dioxide ($scCO_2$) mediated reactions.

Our group recently developed a simple approach for the preparation of well-ordered block copolymer/NP composites through additive-driven self-assembly.[5,6,18] This approach uses multipoint, enthalpically favorable interactions between NPs containing hydrogen bond donating ligands with hydrogen bond accepting block copolymer segments. These enthalpically favorable interactions enable the preparation of highly filled, well-ordered composites and, in some cases, allows otherwise disordered block copolymer templates to form ordered block copolymer morphologies.

To produce well-ordered mesoporous silica films containing high-loadings of NPs, we use these highly filled composites as solid templates in a three-dimensional (3-D) replication process that has been reported by our group earlier.[19–23] This process relies on the dilation of block copolymer templates in supercritical carbon dioxide ($scCO_2$) and high solubility of silica precursors such as silicon alkoxides in $scCO_2$. The block copolymer thin film templates are typically prepared by spin-coating amphiphilic block copolymer solutions containing catalytic amounts of organic acid. The amphiphilic block copolymer template is then exposed to a humidified $scCO_2$ solution of a silica precursor such as silicon alkoxides. During phase separation of the template, the organic acid partitions within the hydrophilic domains of the template such that upon introduction of $scCO_2$, hydrolysis and condensation of the precursor to form the silica network occurs exclusively within

Polymer Science and Engineering Department, University of Massachusetts Amherst, Conte Center for Polymer Research, 120 Governors Drive, Amherst, MA, USA. E-mail: watkins@polysci.umass.edu; Fax: +1-413-545-0082; Tel: +1-413-545-2569

† Electronic supplementary information (ESI) available: Experimental results for the incorporation of gold (Au) NPs within mesoporous silica matrix. See DOI: 10.1039/c4tc00406j

‡ These authors equally contributed to the work.

the hydrophilic domain of the template. The unmodified hydrophobic domains of the template subsequently generate the mesopore, *i.e.* the chemistry is phase selective. The use of $scCO_2$ allows for the amphiphilic block copolymer template to be dilated sufficiently, increasing the penetrate diffusion rates[24] and permitting uniform infiltration of the silica precursors within the template. The infused silica/block copolymer composite is then subjected to calcination at 400 °C to remove the polymer template and yield a mesoporous silica thin film. The size and the shape of the domain level structure of the well ordered hybrid materials can be easily modified by changing the block copolymer molecular weight or by changing the relative volume fractions of the blocks. The $scCO_2$ processing scheme described here separates the ordering of the block copolymer template from the inorganic matrix formation which allows adjustments to be made to the template before the silica network is established. This separation of template formation and inorganic matrix establishment also allows for the block copolymer template to be lithographically patterned using chemically amplified deprotection methods, which imparts 2-D device level surface patterning simultaneously with mesopore formation.[25,26] Here the preparation of highly filled block copolymer/NP composite templates *via* additive driven assembly followed by phase selective silica condensation within the block copolymer domain containing the NPs enables the synthesis of mesoporous silica films with pore walls containing high concentrations of NPs.

2. Experimental section

2.1 Materials

4-Hydroxybenzoic acid (99%, Acros Organics), oleylamine (approximate C18-content 80–90%, Acros Organics), oleic acid (97%, Acros Organics), dioctyl ether (99%, Sigma Aldrich), iron(0) pentacarbonyl (>99.99%, trace metals basis, Sigma Aldrich), platinum(II) acetylacetonate (97%, Sigma Aldrich), trioctylphosphine (97%, Sigma Aldrich), 1,2-hexadecanediol (>98%, TCI America), hydrogen tetrachloroaurate trihydrate (MP Biomedical, ACS Grade), *para*-mercaptophenol (Acros Organic, 99%), acetic acid (Fisher Scientific, Glacial), sodium borohydride (Aldrich, Venpure SF), Pluronic® F127 (EO_{106}-PO_{70}-EO_{106}) block copolymer (BASF), *para*-toluene sulfonic acid (99%, Acros Organics), tetraethyl orthosilicate (99.999%, Sigma Aldrich), and carbon dioxide (CO_2, Merriam Graves, bone-dry grade) were used as received without further purification. Common solvents were purchased from Fisher Scientific and were used as received without further purification. Silicon wafers of (100) orientation (p-type, boron dopant) were obtained from University Wafer.

2.2 Iron platinum (FePt) nanoparticle synthesis

The synthesis of monodisperse hydrophobic FePt NPs was based on the method previously reported by Sun *et al.*[27] The resulting alkyl-functionalized NPs formed stable dispersions in solvents with low polarity such as alkanes, alkenes and chlorinated solvents. These NPs were employed as the starting material for the preparation of hydrophilic NPs through a simple one-step ligand exchange reaction with small-molecule ligands such as 4-hydroxybenzoic acid. Typically, as-synthesized FePt NP solid was mixed with 10× hydrophilic ligand (by weight) in a 20 mL scintillation vial with the targeting solvent (*e.g.* ethanol). The reaction was facilitated by 10 minutes of sonication and 1 hour of magnetic stirring to ensure a satisfactory yield. The vial appeared to be dark yet transparent in just a few minutes, indicating a fast reaction rate. The exchanged FePt NPs were than precipitated out with the addition of successive anti-solvent (*e.g.* hexanes) and collected with centrifugation operating at 5k RPM for 5 minutes. The resulting NP powders were readily dispersed in polar solvent (such as alcohols, tetrahydrofuran (THF), and dimethylformamide (DMF)) and remained stable during long period of observation (> 1 year). The same purification procedures were applied as necessary until all the excessive ligands were removed. Detailed information of this ligand exchange method and properties of the hydrophilic magnetic nanoparticle are reported elsewhere.

2.3 Silicon wafer preparation

Silicon substrates ($1'' \times 1''$) were cleaned by ultrasonication in concentrated sulfuric acid (H_2SO_4, Fisher Scientific, ACS Grade) for 15 minutes followed by rinsing with acetone (Fisher Scientific, ACS Grade) and isopropyl alcohol (Fisher Scientific, ACS Grade) and dried under a stream of nitrogen (N_2).

2.4 Supercritical carbon dioxide processing

Mesoporous silica films doped with NPs were prepared by exposing the amphiphilic block copolymer templates doped with FePt NPs to a solution of tetraethyl orthosilicate (TEOS) in supercritical carbon dioxide ($scCO_2$) within a high pressure reactor at 60 °C and 125 bar. The high pressure reactor, ~160 mL in volume, is constructed from two stainless steel opposed ended hubs sealed with a graphite ring (55 ft lb torque) purchased from Grayloc® Products. Heating bands (Watlow®) are connected to the outside of the reactor walls to control the gas temperature. The top reactor hub is drilled to have 4 ports; one to measure internal pressure, one to measure internal temperature, one for gas inlet and one for gas outlet. For the Pluronic® F127 solution containing pre-synthesized NPs, 20 μL of TEOS was directly placed within the high pressure reactor along with 300 μL of deionized water, each in separate Vespel® containers, prior to sealing. Once the reactor was sealed and heated to a gas temperature of 60 °C, an equilibrium time of 2 hours was observed to allow the polymer templates sufficient annealing and water uptake. CO_2 was injected with a high pressure syringe pump (ISCO, Model 500 HP) at a rate of 2–3 mL min^{-1}. Once the correct pressure was reached, a soak time of 2 hours at 60 °C and 125 bar was observed. The reactor was then de-pressurized within 20 minutes to ambient pressure. Samples were thermally degraded at 400 °C for 6 hours with a ramp rate of 1.56 °C min^{-1}.

2.5 Characterization

Film thicknesses were measured with a Filmetrics F20 Thin Film Measurement System and reported values were an average

of 5 measurements over the entire surface with a deviation of ±5 nm. Transmission electron microscopy (TEM) samples were prepared by scraping mesoporous silica from the substrate, grinding *via* mortar and pestle, suspended with ethanol and transferred to a holey-carbon-coated copper grid to be analyzed with a JEOL 2000FX II operating at 200 kV. High resolution TEM (HRTEM) was performed with a JEOL 2010 operating at 200 kV. Field Emission Scanning Electron Microscope (FESEM), operating in scanning transmission electron microscopy (STEM) mode, was performed with a FEI Magellan 400 operating at 5 kV. X-ray diffraction (XRD) and low-angle XRD (LAXRD) were performed on a PANalytical X'Pert diffractometer, using copper (Cu) Kα X-rays (0.1542 nm) operating at 45 kV and 40 mA. Ultraviolet-visible (UV-Vis) spectra were obtained on an Agilent 8453 UV-Vis spectrometer and collected with an integration time of 0.5 seconds and intervals of 1 nm. X-ray photoelectron spectroscopy (XPS) measurements were conducted on a Quantum 2000 scanning electron spectroscopy for chemical analysis (ESCA) microprobe (Physical Electronics, Inc.) using Al Kα radiation (1486.6 eV). Survey spectrums were acquired in the binding energy range of 0–1100 eV using 187 eV pass energy and 1.6 eV step size. For depth comparison analysis, samples were sputtered with an argon (Ar+) ion-sputtering gun operating at 1 keV and 20 nA. After each sputtering event, narrow scans were acquired using pass energy and step size of 46.9 eV and 0.2 eV respectively. Raw XPS data was analyzed using MultiPak V6.1A (Physical Electronics, Inc.) software.

3. Results and discussion

The Pluronic® family of block copolymers are amphiphilic triblock copolymers that consist of hydrophilic poly(ethylene oxide) (PEO) and hydrophobic poly(propylene oxide) (PPO) segments. To incorporate significant weight fractions of pre-synthesized FePt NPs into the Pluronic® block copolymer, a favorable interaction between the pre-synthesized NP and Pluronic® PEO segment must be established. We recently demonstrated that high loadings of pre-synthesized metal and semiconducting NPs located within the PEO segments of Pluronic® copolymers could be achieved to yield well-ordered composites by exploiting strong interactions between the NP ligands and the PEO segment. For example, Lin *et al.*, showed that gold (Au) NPs decorated with *para*-mercaptophenol as the hydrogen bond donating ligand increased the segregation strength and enabled Au NP loadings as high as 30 wt% in the well-ordered composite.[5] This strategy has been further extended to incorporate similar loadings of FePt NPs decorated with the hydrogen bond donating 4-hydroxybenzoic acid within the PEO segment of Pluronic® F127, PEO_{106}-*b*-PPO_{70}-*b*-PEO_{106}, copolymer template which is known to phase separate into a cylindrical morphology, both in bulk[28,29] and thin film samples.[30]

Fig. 1 illustrates how the desired mesoporous silica doped with pre-synthesized NPs was produced. The process begins by spin-coating a solution of NPs (pre-synthesized FePt NPs of ~2–3 nm in diameter as shown in Fig. 2) with Pluronic® F127 and *para*-toluene sulfonic acid (PTSA), which is a strong organic

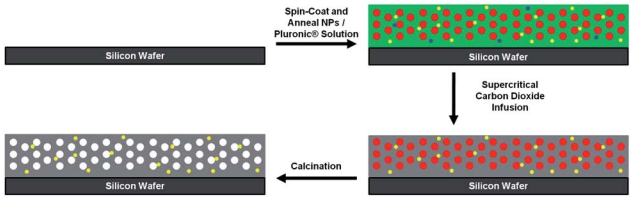

Fig. 1 Illustration showing the fabrication steps to create mesoporous silica doped with gold nanoparticles.

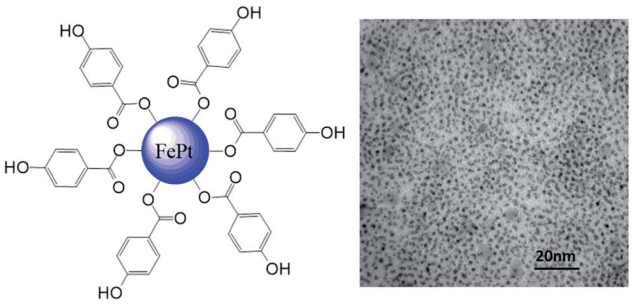

Fig. 2 Cartoon depicting the FePt NPs decorated with 4-hydroxybenzoic acid ligands (left). TEM image of the as synthesized FePt nanoparticles functionalized with 4-hydroxybenzoic acid ligands (right) with a particle size of ~2 nm.

acid used to promote the hydrolysis and condensation of the silica network, to create 400–500 nm thin films. The solutions consisted of 10 wt% solids (Pluronic® F127, pre-synthesized NPs and PTSA) and 90 wt% DMF solvent for the case of FePt NPs. Concentration of the pre-synthesized NPs ranged from 5 wt% to 25 wt% with respect to Pluronic® F127 while the concentration of the PTSA was held constant at 15 wt% with respect to all solid materials. The solutions were stirred at room temperature for 15 minutes to ensure the components were sufficiently mixed. The solutions were then directly spin-coated in an air environment, through a 0.2 μm poly(tetrafluoroethylene) (PTFE) filter, on a cleaned silicon wafer for 90 seconds at 3000 rpm. The thin films showed no signs of crystallization, de-wetting or macro-phase separation.

To template the mesoporous silica around the pre-synthesized NPs, the thin film samples were exposed to a humidified solution of $scCO_2$ containing the silicon alkoxide precursor of tetraethyl orthosilicate (TEOS) at 60 °C and 125 bar for 2 hours. The unique aspect of templating mesoporous silica through the use of $scCO_2$ processing is that the thin film block copolymer template formation is separated from the condensation of the silica precursor. This allows the block copolymer template to retain the morphology created during the spin-coating and annealing steps and remain unperturbed during the formation of the silica network. Generation of the mesopores and removal of organic material is simultaneously achieved by thermal degradation. Calcination was performed with a 1.56 °C min^{-1} ramp rate from room temperature to 400 °C, held at 400 °C for 6 hours and brought back to room temperature with a ramp rate of 1.56 °C per min^{-1}. Fabrication of mesoporous silica through the $scCO_2$ processing has also been characterized to show that

an interpenetrating network (IPN) structure is formed from the micropores created during the thermal degradation of the PEO blocks.[31] Such characteristics of the mesoporous silica, *i.e.* high degree of wall porosity, created through $scCO_2$ processing, once doped with pre-synthesized NPs, make for unique substrates that are ideal for use in catalysis and sensing applications.

Mesoporous silica samples containing pre-synthesized FePt NPs of 5 wt% and 25 wt%, with respect to the Pluronic® F127 template, were created. X-ray diffraction (XRD) was used to evaluate the structure of the mesoporous silica/NP composites and the data is provided in Fig. 3. For composites containing silica/NPs/polymer, a well-ordered hexagonal structure was observed with domain spacing between 13.8 nm and 14.0 nm.

When the polymer material was removed from the composite, yielding only mesoporous silica and NPs in the composite, a well-ordered hexagonal structure was observed but the domain spacing was reduced to between 10.9 nm and 11.6 nm. The difference between the domain spacings between the uncalcined and calcined samples corresponds to the shrinkage in the lattice parameters, by ~20%, due to removal of the polymer template and organic material (*e.g.* NP ligands) as well as further condensation of the silica matrix. Also, the increase in scattering intensity in the composite without the polymer template, when compared to the composite with the polymer template, is as expected due to the greater differences in electron density between the two composites, *i.e.* upon removal of the minor block copolymer domains to yield the mesopores.

Electron microscopy was used to confirm the presence of the NPs within the mesoporous silica. The transmission electron microscopy (TEM) image in Fig. 4a shows the successful incorporation of pre-synthesized NPs into mesoporous silica while maintaining the presence of mesopores with diameters between 5–6 nm for mesoporous silica samples containing 25 wt% of pre-synthesized NPs. The darkest areas of the electron micrographs correspond to the NPs, while the lighter gray areas correspond to the silica and the white areas correspond to the mesopores. A higher magnification TEM image, provided in Fig. 4b and c, confirms the presence of NPs and suggests that the NPs are predominately located within the mesopore walls rather than in the mesopores themselves. This partitioning of NPs within the mesoporous silica walls is consistent with the initial partitioning of NPs within the hydrophilic (PEO) segment of the Pluronic® block copolymer template, only now the hydrophilic segment of the Pluronic® block copolymer template is infused with silica from the hydrolysis and condensation of TEOS during $scCO_2$ processing. There is no evidence of coarsening or aggregation of the FePt NPs during calcination, indicating that the particles are stable and remain well distributed during template removal and further silica network condensation. X-ray photoelectron spectroscopy (XPS)

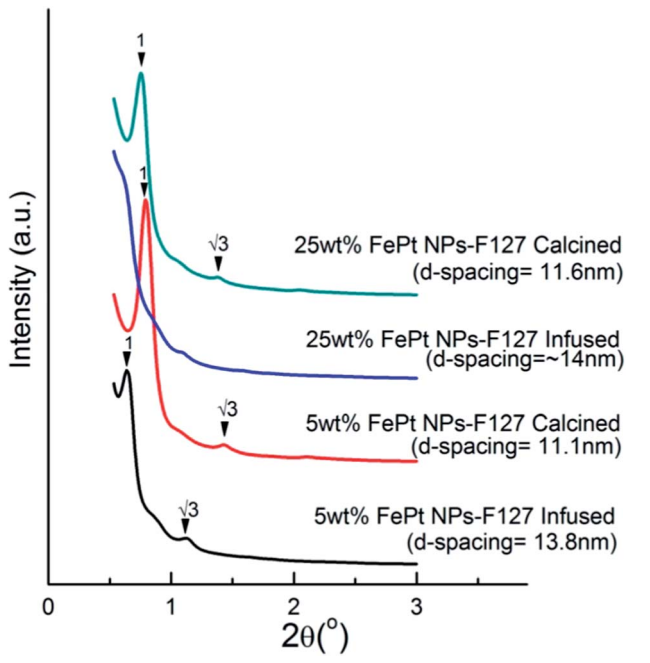

Fig. 3 Low-angle X-ray diffraction (LAXRD) for mesoporous silica containing pre-synthesized FePt NPs. Weight percent of FePt NPs is with respect to Pluronic® F127. The terms of infused and calcined refer to the presence of organic materials (infused) and to the presence of no organic material (calcined).

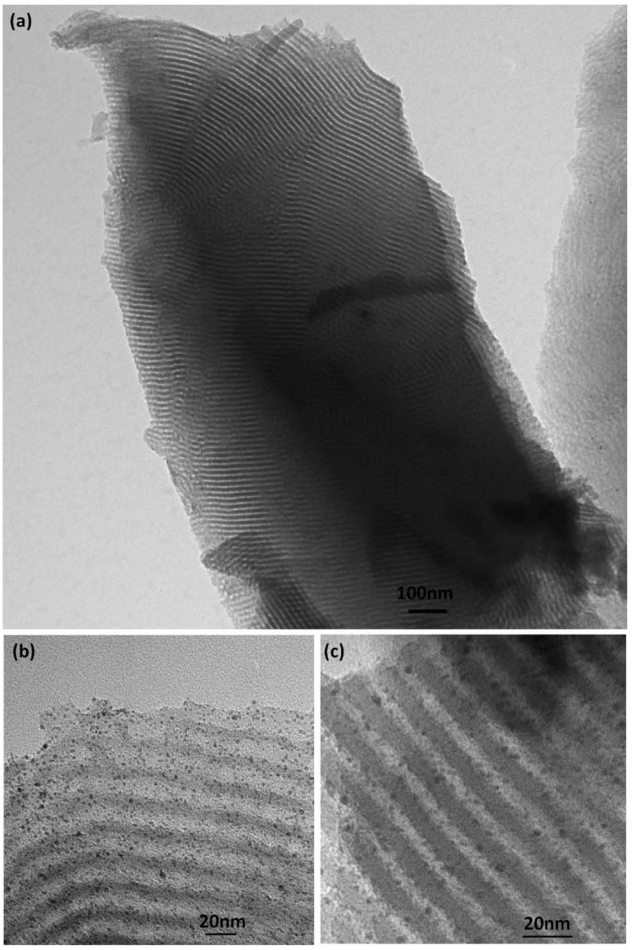

Fig. 4 TEM images of mesoporous silica created from Pluronic® F127 containing 25 wt% pre-synthesized FePt NPs (a) low magnification image showing presence of cylindrical mesopores (b and c) high magnification images displaying FePt NPs within mesoporous silica.

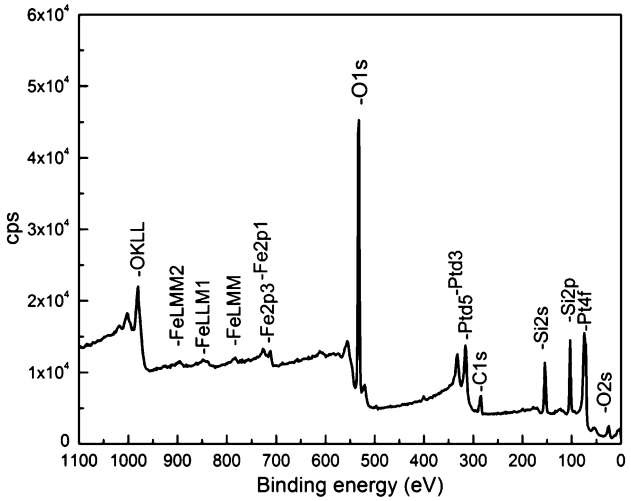

Fig. 5 XPS survey spectrum of mesoporous silica created from Pluronic® F127 template containing 25 wt% pre-synthesized FePt NPs.

survey spectrum (Fig. 5) of mesoporous silica created from Pluronic® F127 template containing 25 wt% pre-synthesized FePt NPs show Auger and photoelectron features of silicon (Si), oxygen (O), iron (Fe) and platinum (Pt) along with carbon (C) as an impurity on the surface. Fig. 6 shows specific scans of these elements after sputtering for the time indicated in the legend. Composition analysis after each sputtering event confirms the presence of NPs in the bulk of the film. No carbon impurity was observed after the first 30 seconds of sputtering. Composition profiles with sputtering times are plotted in Fig. 7 where the average FePt NPs concentration in the bulk of the film, with respect to mesoporous silica, was determined to be 15 wt%.

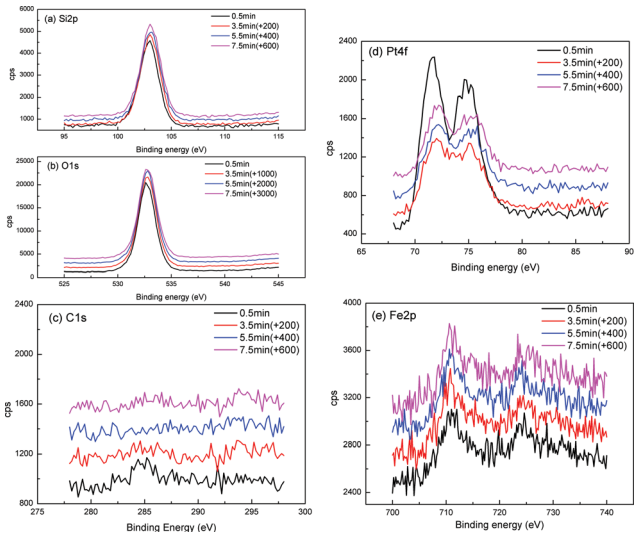

Fig. 6 Specific scans of mesoporous silica created from the Pluronic® F127 template containing 25 wt% pre-synthesized FePt NPs after different sputtering times: (a) Si2p; (b) O1s; (c) C1s; (d) Pt4f; (e) Fe2p. Legend represents the sputtering time prior to data acquisition. Number in the bracket next to legend is shift in *Y*-axis for clear representation.

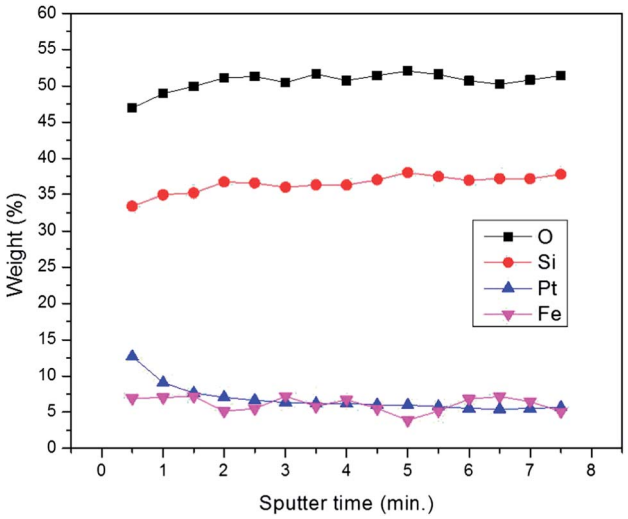

Fig. 7 XPS composition profiles *vs.* sputtering time for mesoporous silica created from Pluronic® F127 template containing 25 wt% pre-synthesized FePt NPs.

This is consistent with the presence of the ligands on the FePt NPs and replacement of the low density Pluronic® F127 template with the higher density silica matrix. We also evaluated the incorporation of gold (Au) NPs within mesoporous silica using this approach. While high loadings of NPs were achieved, the high temperatures used for calcination and the low melting point of Au NPs lead to ripening and growth of the Au NPs. These results are provided in the ESI.†

4. Conclusions

We present a method for the preparation of mesoporous silica/NP composites containing high concentrations of NPs within the silica walls. FePt NPs of 2–3 nm diameters decorated with 4-hydroxybenzoic acid ligands selectively hydrogen bond to the hydrophilic segment of Pluronic® F127 enabling the generation of templates with high concentration of NPs located selectively within the PEO domain. The NPs were then encapsulated by the generation of silica *via* phase selective hydrolysis and condensation of TEOS to form silica within the PEO/NP domain of the composite template while swollen with $scCO_2$. Calcination removed both the template and the NP ligands yielding NP doped mesoporous silica. X-ray scattering confirmed the presence of hexagonally ordered mesopores in the silica/NP composites. Electron microscopy confirmed that the NPs reside primarily within the walls of the mesoporous silica allowing the mesopores to be free of obstruction to the transport of materials. At a FePt NPs loading of 25 wt%, with respect to the Pluronic® template, the FePt NPs were stable during preparation of the mesoporous silica and remained well dispersed and less than 3 nm in diameter. The procedure described here could be applied to any number of NPs, although ripening may be observed during calcination for NPs with low melting points. In the latter case, other means of template removal, such as plasma processing, may be required.

Acknowledgements

Funding for this research was provided by the National Science Foundation through the Center for Hierarchical Manufacturing (CHM, CMMI-0531171) at the UMass Amherst and a NIST/GRC Graduate Fellowship to N. R. Hendricks. HRTEM work was conducted in the labs of Professor Richard Tilley at the MacDiarmid Institute, Victoria University of Wellington, New Zealand. N. R. Hendricks would like to acknowledge assistance with HRTEM from Alec La Grow and with nanoparticle synthesis from Dr. Ying Lin.

Notes and references

1 C. Burda, X. Chen, R. Narayanan and M. A. El-Sayed, *Chem. Rev.*, 2005, **105**, 1025–1102.
2 S. Gupta, Q. Zhang, T. Emrick, A. C. Balazs and T. P. Russell, *Nat. Mater.*, 2006, **5**, 229–233.
3 J.-Y. Lee, Q. Zhang, T. Emrick and A. J. Crosby, *Macromolecules*, 2006, **39**, 7392–7396.
4 Q. Li, J. He, E. Glogowski, X. Li, J. Wang, T. Emrick and T. P. Russell, *Adv. Mater.*, 2008, **20**, 1462–1466.
5 Y. Lin, V. K. Daga, E. R. Anderson, S. P. Gido and J. J. Watkins, *J. Am. Chem. Soc.*, 2011, **133**, 6513–6516.
6 V. K. Daga, E. R. Anderson, S. P. Gido and J. J. Watkins, *Macromolecules*, 2011, **44**, 6793–6799.
7 M. Haruta, S. Tsubota, T. Kobayashi, H. Kageyama, M. J. Genet and B. Delmon, *J. Catal.*, 1993, **144**, 175–192.
8 T. Hayashi, K. Tanaka and M. Haruta, *J. Catal.*, 1998, **178**, 566–575.
9 R. Zanella, S. Giorgio, C. R. Henry and C. Louis, *J. Phys. Chem. B*, 2002, **106**, 7634–7642.
10 A. K. Sinha, S. Seelan, S. Tsubota and M. Haruta, *Angew. Chem., Int. Ed.*, 2004, **43**, 1546–1548.
11 A.-H. Lu, W. Schmidt, N. Matoussevitch, H. Bönnemann, B. Spliethoff, B. Tesche, E. Bill, W. Kiefer and F. Schüth, *Angew. Chem.*, 2004, **43**, 4303–4306.
12 S. C. Tsang, V. Caps, I. Paraskevas, D. Chadwick and D. Thompsett, *Angew. Chem.*, 2004, **43**, 5645–5649.
13 B. J. Wang, *Proc. IEEE*, 2008, **96**, 1847–1863.
14 D. Kami, S. Takeda, Y. Itakura, S. Gojo, M. Watanabe and M. Toyoda, *Int. J. Mol. Sci.*, 2011, **12**, 3705–3722.
15 W. Wu, D. Caruntu, A. Martin, M. H. Yu, C. J. O'Connor, W. L. Zhou and J.-F. Chen, *J. Magn. Magn. Mater.*, 2007, **311**, 578–582.
16 D. M. Hess, R. R. Naik, C. Rinaldi, M. M. Tomczak and J. J. Watkins, *Chem. Mater.*, 2009, **21**, 2125–2129.
17 A. Zeleňáková, J. Kováč and V. Zeleňák, *J. Appl. Phys.*, 2010, **108**, 034323.
18 A. H. Romang and J. J. Watkins, *Chem. Rev.*, 2010, **110**, 459–478.
19 R. A. Pai, R. Humayun, M. T. Schulberg, A. Sengupta, J.-N. Sun and J. J. Watkins, *Science*, 2004, **303**, 507–510.
20 R. A. Pai and J. J. Watkins, *Adv. Mater.*, 2006, **18**, 241–245.
21 V. R. Tirumala, R. A. Pai, S. Agarwal, J. J. Testa, G. Bhatnagar, A. H. Romang, C. Chandler, B. P. Gorman, R. L. Jones, E. K. Lin and J. J. Watkins, *Chem. Mater.*, 2007, **19**, 5868–5874.
22 S. Nagarajan, M. Li, R. A. Pai, J. K. Bosworth, P. Busch, D.-M. Smilgies, C. K. Ober, T. P. Russell and J. J. Watkins, *Adv. Mater.*, 2008, **20**, 246–251.
23 N. R. Hendricks, J. J. Watkins and K. R. Carter, *J. Mater. Chem.*, 2011, **21**, 14213–14218.
24 R. R. Gupta, V. S. RamachandraRao and J. J. Watkins, *Macromolecules*, 2003, **36**, 1295–1303.
25 S. Nagarajan, J. K. Bosworth, C. K. Ober, T. P. Russell and J. J. Watkins, *Chem. Mater.*, 2008, **20**, 604–606.
26 H.-T. Chen, T. A. Crosby, M.-H. Park, S. Nagarajan, V. M. Rotello and J. J. Watkins, *J. Mater. Chem.*, 2009, **19**, 70.
27 A. Sun, S. Murray, C. B. Weller, D. Folks and L. Moser, *Science*, 2000, **287**, 1989–1992.
28 V. R. Tirumala, A. Romang, S. Agarwal, E. K. Lin and J. J. Watkins, *Adv. Mater.*, 2008, **20**, 1603–1608.
29 V. R. Tirumala, V. Daga, A. W. Bosse, A. Romang, J. Ilavsky, E. K. Lin and J. J. Watkins, *Macromolecules*, 2008, **41**, 7978–7985.
30 V. K. Daga and J. J. Watkins, *Macromolecules*, 2010, **43**, 9990–9997.
31 B. D. Vogt, R. A. Pai, H.-J. Lee, R. C. Hedden, C. L. Soles, W. Wu, E. K. Lin, B. J. Bauer and J. J. Watkins, *Chem. Mater.*, 2005, **17**, 1398–1408.